

Theoretical studies on electronic structure and properties of type I copper center in copper proteins

著者	Kurniawan Isman, Kawaguchi Kazutomo, Sugimori Kimikazu , Sakurai Takeshi, Nagao Hidemi
著者別表示	川口 一朋, 杉森 公一, 櫻井 武 , 長尾 秀実
journal or publication title	The Science Reports of Kanazawa University
volume	63
page range	1-13
year	2019
URL	http://doi.org/10.24517/00055866



Theoretical studies on electronic structure and properties of type I copper center in copper proteins

Isman KURNIAWAN,^{1,2*} Kazutomo KAWAGUCHI,¹ Kimikazu SUGIMORI,³
Takeshi SAKURAI,⁴ Hidemi NAGAO¹

¹Division of Mathematical and Physical Sciences, Graduate School of Natural Science and Technology,
Kanazawa University, Kanazawa 920-1192, Japan

²School of Computing, Telkom University, 40257, Indonesia

³Division of Higher Education Research and Development, Institute of Liberal Arts and Science,
Kanazawa University, Kanazawa 920-1192, Japan

⁴Division of Material Chemistry, Graduate School of Natural Science and Technology,
Kanazawa University, Kanazawa 920-1192, Japan

(Received August 8, 2018 and accepted in revised form October 29, 2018)

Abstract We present a cluster model representing type I copper (T1Cu) center of copper protein, which corresponds to Multicopper Oxidases, Azurin, Stelacyanin and so on. The electronic structure and physical properties such as molecular orbital, atomic partial charge, partial spin densities, ionization energy (IP) of reduced T1Cu, electron affinity (EA) of oxidized T1Cu, the bond and the angle constants etc. are calculated by using two typical Density Functional Theory (DFT) functionals, which are B3LYP and M06, with 6-31G(d) basis set. We find the dependency of several properties such as atomic partial charge, partial spin densities, IP, and EA on the DFT functionals. We also find that the DFT functionals give a better contribution to bond constants, especially in case of the interaction between copper and the axial ligand. We calculate the maximum absorption wavelength of T1Cu center and find relatively a good agreement with experimental data.

Keywords. Type I copper center, density functional theory, electronic structure.

1 Introduction

Copper proteins play an important role in various biological processes such as electron transfer, redox reaction, oxygen transportation, activation and so on. The proteins can contain one or more copper ions in their active sites. Copper proteins containing one copper ion are known as type I copper (T1Cu) protein, such as Azurin, Plastocyanin, Stelacyanin and so on, and copper proteins containing more than two copper ions are known as Multicopper Oxidases (MCOs). MCOs contain two copper centers, which are T1Cu center and tri-nuclear copper (TNC) center, in which those centers are located at different sites. T1Cu center consists of one copper ion coordinated to two histidines and a cysteine in a trigonal planar structure, and an axial ligand such as methionine

*Corresponding author Email: isman@wiron1.s.kanazawa-u.ac.jp

and so on [1–3]. T1Cu center catches one electron from other proteins with higher redox potential and transfer the electron to the TNC site [4–6]. During the reaction, dioxygen molecules are reduced to two water molecules in TNC site by using the transferring four electrons from T1Cu [7].

Many physical properties such as electronic structure, reaction, etc. of T1Cu have been experimentally investigated by many groups [7–12]. The existence of T1Cu has been characterized from intense absorption at around 600 nm and narrow hyperfine splittings in the electron paramagnetic resonance (EPR) spectroscopy [7, 9]. The kinetic aspect of the electron transfer reaction has been investigated by Holwerda and co-workers [8]. They found the dependency of the rate of electron transfer on pH value. Solomon and co-workers have also investigated the room temperature circular dichroism and magnetic circular dichroism spectra of several T1Cu protein such as Stellacyanin, Plastocyanin, and Azurin [9]. Regarding the absorption and circular dichroism intensities, they have pointed out band absorptions as representative of transition energy.

Several physical properties of MCOs have also been investigated by many groups [7, 13–28]. Solomon and coworkers have reviewed some reported physical properties such as electron paramagnetic spectra (EPR) and redox potential of MCOs [13]. The mechanism of oxygen binding and redox reaction on TNC site have also been proposed by several research groups [13, 14, 20, 25]. Roberts and coworkers have investigated the intermolecular and intramolecular electron transfers of MCOs using laser flash photolysis [17]. The direct electron transfer between MCOs and electrode has been investigated by Shleev and coworkers [18]. They found the possibility of the long-range electron transfer between MCOs and electrodes. Augustine and coworkers have also investigated the contribution of the structure of active site in supporting the efficiency of oxygen reduction in TNC [26]. They found that asymmetrical structure of TNC lead to a rapid and efficient reduction reaction.

On the other hand, from the viewpoint of theoretical studies, the electronics structure of T1Cu center has many interests in relation to the electron transfer between molecules. Solomon and co-workers have experimentally and theoretically investigated the electronic structure of T1Cu center in several copper proteins [4, 29]. By quantum mechanical calculations, they presented the X-ray properties of T1Cu center from the viewpoint of the metal-ligand bonding interaction. Corni and co-workers have investigated the contribution of electronic properties of Azurin's active site to electron transfer reaction by using Density Functional methods [30]. They found that in spite of the similarity of the hybridization of azurin in two oxidation states their energy spectrums were found to be different. Other many groups have also investigated the electronic properties and electron transfer mechanism of T1Cu center in copper proteins [31, 32].

In quantum mechanics, density functional methods have been developed to improve the ability in calculating a certain properties of a particular system. Zhao and Truhlar have presented the M06 suite of density functionals [33, 34]. This functional is well known to perform better than B3LYP because of the implementation of meta-GGA functional in exchange-correlation functional of DFT. The M06 functional has been utilized to calculate molecular properties of both organic and inorganic molecules with the promising results [35–37].

In our previous study, we have investigated the electronic structure of the oxidized state of Azurin and have found the dependency of electronic properties on the active site structure [38]. We have also investigated the electronic structure of T1Cu center of Azurin obtained from two stable configuration [39]. The solvent effect on the electronic structure of Azurin's active site has also been investigated by using Polarizable Continuum Model (PCM) [40]. The aim of this study is to investigate the dependency of electronic structure and properties of T1Cu center on DFT functional. We investigate properties such as molecular orbital, atomic partial charge, partial spin densities, ionization energy (IP) of reduced T1Cu, electron affinity (EA) of oxidized T1Cu,

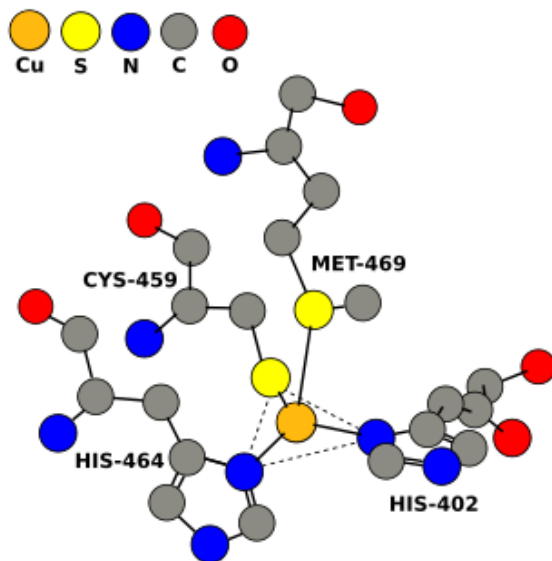


Figure 1: The schematic diagram of Type I copper model cluster.

the bond and the angle constants. Amongst copper proteins containing T1Cu center, we present cluster models for T1Cu center to investigate the physical properties as azurin, stellacyanin, and MCOs as typical examples. Particularly, we discuss the contribution of DFT functional to the properties in relation to the interaction between Cu and ligands.

2 Computational Methods

In this section, we introduce the procedures to calculate the electronic properties and force field parameters of the T1Cu center. We investigate the T1Cu cluster obtained from three copper proteins of Multicopper Oxidase (MCOs), Azurin and Stellacyanin. The cluster model of T1Cu is prepared from the X-ray crystal structure and then the electronic properties of the cluster were calculated. We also estimate force field parameters around T1Cu by using quantum mechanical calculations. The development of the force field parameters of a metal cluster in metalloprotein is required to be able to perform molecular dynamics simulation. The stability of the dynamics around the metal in the cluster corresponds to the quality of the force field parameters. All of the calculations are performed by using Gaussian 09 package [41].

2.1 Cluster Model for the Type I Copper Center

The cluster model of T1Cu is extracted from X-ray crystal structure of three copper proteins. In the case of oxidized state, T1Cu clusters of MCOs, Azurin and Stellacyanin proteins are prepared from the X-ray crystal structure with the PDB ID being 4NER [27], 4AZU [42], and 1X9R [43], respectively. In the case of reduced state, the clusters of MCOs, Azurin and Stellacyanin proteins are prepared from the X-ray crystal structure with the PDB ID being 4E9T [24], 1E5Y [44], and 1X9U [43], respectively. The structure of the T1Cu cluster consists of a copper ion, two histidines, a cysteine, a methionine, and glutamine peptides as shown in Fig. 1. The hydrogen atoms are added into the cluster and are optimized by using B3LYP/6-31G(d) method [38].

2.2 Electronic Properties

Several electronic properties of T1Cu such as molecular orbital, atomic partial charges and partial spin densities are calculated and analyzed. In this study, the atomic partial charges are estimated by using Merz-Singh-Kollman scheme [45]. We also calculate other properties such as ionization potential (IP) of reduced T1Cu, electron affinity (EA) of oxidized T1Cu and maximum absorption wavelength. The maximum absorption wavelengths are calculated by using time-dependent density functional theory (TD-DFT) method combined with conductor-like polarizable continuum model (CPCM). The value of ϵ is taken as 10 [46,47] and Topological United Atoms model was used as atomic radii.

2.3 Force Field Parameters

To determine the force field parameters, we calculate the total energies of T1Cu with several values of bond and angle distance by using B3LYP and M06. The bond distance is varied in the range of $\pm 0.1 \text{ \AA}$ from equilibrium distance with increment 0.02 \AA , while angle distance is varied in the range of $\pm 5^\circ$ from equilibrium angle with increment 1° [48]. The value of total energy is used to construct a potential energy surface (PES) along the bond distance and angle. The curvature of PES is fitted by using harmonic potential function, which is represented as ([38])

$$V(r, K_r) = K_r(r - r_c)^2, \quad (2.1)$$

$$V(\theta, K_\theta) = K_\theta(\theta - \theta_c)^2, \quad (2.2)$$

where K_r and K_θ represent the bond and angle constants, respectively, while r_c and θ_c represent the equilibrium bond and angle, respectively.

3 Results and Discussions

In this section, we present several properties of T1Cu obtained from several copper proteins. Several properties of T1Cu such as atomic partial charge, partial spin densities, ionization potential, electron affinity, maximum absorption wavelength, bond and angle constants are discussed in relation to the dependency of those properties on DFT functional.

3.1 Electronic Properties

Firstly, we present a singly occupied molecular orbital (SOMO) of T1Cu in MCOs protein calculated by using M06, as shown in Fig. 2a. The shape of SOMO is mainly arised from $d_{x^2-y^2}$ orbital of the copper ion, p orbitals of the sulfur and σ orbital of two nitrogen atoms. We find antibonding orbitals in the interaction between copper ion and cysteine's sulfur, two histidine's nitrogen. The orbital of methionine's sulfur is not observed in the SOMO orbital indicating weak interaction between copper ion and methionine residue. The shape of SOMO orbital is found to be similar to the SOMO orbital of T1Cu presented in Ref. [4,39].

The surface of spin density presented in Fig. 2b was calculated by using M06. The shape of the surface is similar to SOMO orbital shown in Fig. 2a, which is a good agreement with our previous study [39]. To obtain a detail information about spin properties, we present atomic partial spin around T1Cu as shown in Table 1. Regarding DFT functional dependency, the partial spin density on the copper ion by M06 is smaller than that by B3LYP. These results are consistently found in all T1Cu cluster indicating that M06 produces partial spin density that is more delocalized around

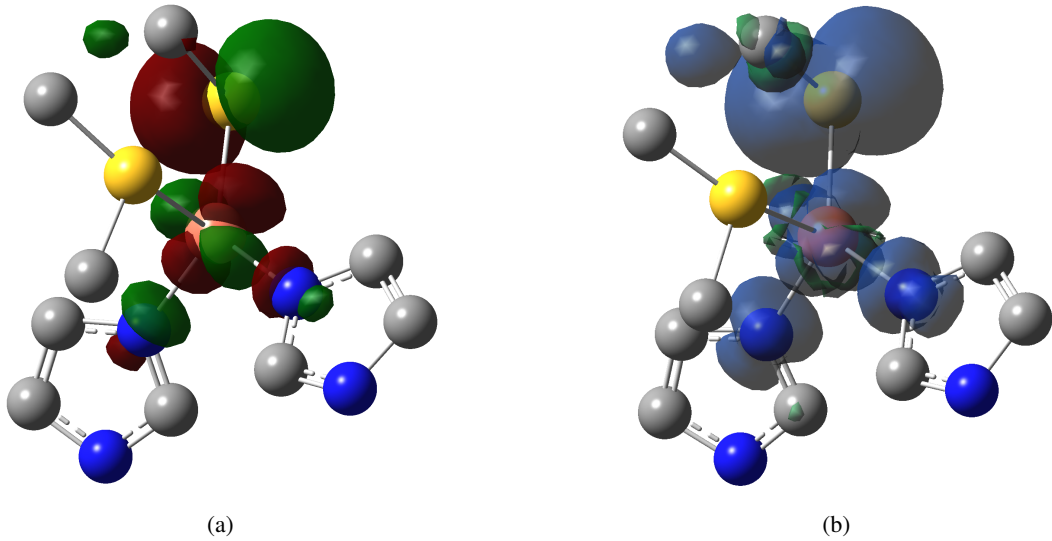


Figure 2: The profile of (a) SOMO orbital and (b) spin density of oxidized type I copper cluster.

Table 1: The atomic spin distribution of oxidized state of type I copper center in several proteins calculated by using B3LYP (M06) methods.

Atom	Atomic Spin Distribution		
	MCOs	Azurin	Stellacyanin
Cu	0.53 (0.49)	0.49 (0.46)	0.57 (0.54)
S ₁	0.38 (0.41)	0.43 (0.47)	0.33 (0.35)
S ₂ /O	0.00 (0.00)	0.00 (0.00)	0.00 (0.00)
N ₁	0.04 (0.04)	0.03 (0.03)	0.05 (0.05)
N ₂	0.19 (0.16)	0.03 (0.03)	0.04 (0.05)

MCOs and Azurin

Stellacyanin

copper ion. The delocalization implies that transfer integral between d -orbital on the copper ion and p -orbital on the sulfur ion in cysteine is larger when M06 is adopted.

Our finding can be related to t/U ratio in simple Hubbard model. This ratio can be used to determine which is the more dominant factor between transfer integral (t) and on-site repulsion (U) in the electron transfer process in copper protein. The large value of t/U ratio indicates the transfer integral is more dominant and vice versa. In our results, the decreasing of the partial spin density of copper ion, that indicate the delocalization of unpaired electron, lead to an increase of t/U ratio. This implies that the transfer integral is more dominant in our calculation. We find a result related to the t/U ratio that is similar to our previous study [38]. Atomic partial spin of methionine's sulfur is found to be zero in all T1Cu cluster. This indicates that the probability of unpaired electron of copper to be distributed to methionine's sulfur is zero. The large distance between both atoms is the main reason of the zero distribution of unpaired electron around methionine's sulfur.

The distribution of atomic partial charge around T1Cu calculated by using B3LYP and M06 is shown in Table 2. Here, we present the atomic partial charge of all atoms of T1Cu cluster in oxidized and reduced state. However, for the analysis purpose, we focus on the atomic partial charge of the copper ion and the cysteine's sulfur atom because the bond between both atoms is crucial in electron transfer process. We find that M06 calculation produces the partial charge of the copper ion that is less positive and the partial charge of cysteine's sulfur atom that is less negative than that of B3LYP calculation. The tendency is consistently found in all T1Cu clusters. This

Table 2: The atomic partial charge of type I copper center in several proteins calculated by using B3LYP (M06) methods.

Atom	Atomic Partial Charge					
	MCOs		Azurin		Stellacyanin	
	Ox	Red	Ox	Red	Ox	Red
Cu	+0.55 (+0.54)	+0.36 (+0.33)	+0.63 (+0.59)	+0.36 (+0.31)	+0.54 (+0.50)	+0.33 (+0.28)
S ₁	-0.45 (-0.41)	-0.71 (-0.68)	-0.49 (-0.45)	-0.78 (-0.75)	-0.58 (-0.55)	-0.79 (-0.75)
S ₂ /O	-0.22 (-0.23)	-0.21 (-0.22)	-0.40 (-0.38)	-0.34 (-0.32)	-0.61 (-0.61)	-0.60 (-0.60)
N ₁	-0.35 (-0.37)	-0.20 (-0.21)	-0.26 (-0.28)	-0.22 (-0.22)	-0.03 (-0.03)	-0.07 (-0.07)
N ₂	+0.19 (+0.16)	-0.06 (-0.05)	+0.24 (+0.20)	+0.21 (+0.19)	+0.23 (+0.22)	+0.18 (+0.17)
N ₃	-0.17 (-0.18)	-0.36 (-0.36)	-0.29 (-0.26)	-0.26 (-0.23)	-0.26 (-0.27)	-0.31 (-0.30)
N ₄	+0.10 (+0.10)	+0.15 (+0.14)	+0.19 (+0.16)	+0.18 (+0.16)	+0.18 (+0.17)	+0.12 (+0.10)
C ₁	+0.16 (+0.18)	+0.19 (+0.21)	+0.12 (+0.16)	+0.08 (+0.10)	+0.05 (+0.06)	+0.04 (+0.06)
C ₂	-0.09 (-0.08)	-0.01 (-0.01)	-0.07 (-0.04)	-0.10 (-0.09)	-0.04 (-0.04)	-0.11 (-0.11)
C ₃	+0.58 (+0.58)	+0.19 (+0.20)	+0.37 (+0.36)	+0.24 (+0.24)	+0.15 (+0.16)	+0.17 (+0.18)
C ₄	+0.19 (+0.20)	+0.12 (+0.14)	+0.09 (+0.11)	+0.08 (+0.09)	+0.10 (+0.11)	+0.10 (+0.12)
C ₅	+0.03 (+0.02)	-0.17 (-0.16)	-0.01 (+0.02)	-0.13 (-0.12)	-0.05 (-0.05)	-0.11 (-0.11)
C ₆	+0.19 (+0.21)	+0.55 (+0.56)	+0.40 (+0.37)	+0.43 (+0.41)	+0.44 (+0.45)	+0.55 (+0.56)
C ₇	+0.17 (+0.14)	+0.12 (+0.09)	+0.18 (+0.14)	+0.14 (+0.10)	+0.11 (+0.08)	+0.01 (-0.02)
C ₈ /N ₅	+0.08 (+0.08)	+0.06 (+0.06)	+0.11 (+0.09)	+0.11 (+0.09)	-0.14 (-0.15)	-0.15 (-0.15)
C ₉	+0.05 (+0.04)	+0.01 (-0.01)	+0.27 (+0.26)	+0.11 (+0.10)	+0.94 (+0.96)	+0.89 (+0.91)

Ox: Oxidized state, Red: Reduced state.

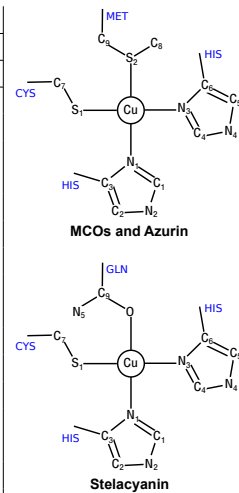


Table 3: The calculation results of ionization potential (IP), electron affinity (EA) and maximum absorption wavelength (λ) of type I copper center in various copper proteins calculated by using B3LYP (M06) methods.

Protein	IP/eV	EA/eV	λ /nm	
			calc.	exp. ^a
Multicopper oxidase	4.86 (5.18)	4.77 (5.02)	661 (672)	610
Azurin	5.04 (5.32)	4.84 (5.12)	684 (695)	631
Stellacyanin	4.87 (5.16)	4.44 (4.71)	577 (580)	609

^a Ref. [4]

finding points out that the negative charge of cysteine's sulfur by M06 is more distributed onto the copper ion and thus affect to the atomic partial charge.

Table 3 shows several physical properties, such as ionization potential (IP), electron affinity (EA), and maximum absorption wavelength (λ) of all T1Cu cluster. The IP and EA values calculated by M06 are found to be consistently larger than those calculated by B3LYP. This indicates the dependency of IP and EA values on DFT functional. We also find that EA value is directly proportional to ligand bond distance shown in Fig. 3. The most significant relationship is found in the bond between copper and cysteine's sulfur that is indicated by a large slope of the curve. This finding implies the significant contribution of this bond in supporting electron transfer process.

Bearing on maximum absorption wavelength, we find that the wavelength calculated by M06 is larger than that calculated by B3LYP. Here, the maximum absorption wavelength represents the transition energy between σ orbital of cysteine's sulfur and $d_{x^2-y^2}$ orbital of copper ion [9]. Meanwhile, the amount of energy required by an electron to move to an orbital with higher energy is defined as band-gap energy. The value of this energy is known to be inversely proportional to the wavelength. As a consequence, the higher value of the wavelength indicates a small value of band-gap energy. In other words, the band-gap energy between σ orbital of cysteine's sulfur and $d_{x^2-y^2}$ orbital of Cu tends by M06 is lower than those by B3LYP.

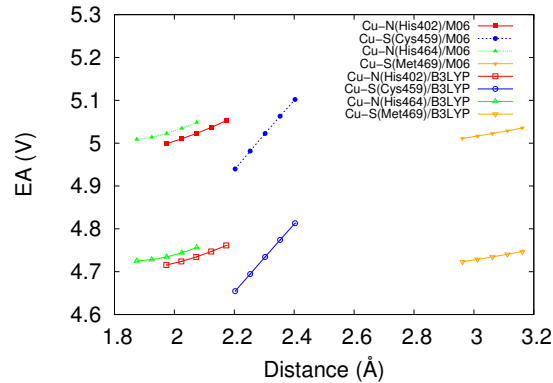


Figure 3: The value of electron affinity as a function of bond distance in T1Cu of MCOs protein. The equilibrium distance is represented by middle point with increment point 0.05 Å.

3.2 Force Field Parameter

The potential energy surfaces (PES) along the bond and angle distance used in fitting procedure are presented in Fig. 4. From fitting analysis, we obtain the bond constant of T1Cu in MCOs, azurin and stellacyanin that are presented in Tables 4, 5 and 6, respectively. We find a significant contribution of DFT functional to the bond constant. The bond constants calculated by M06 are found to be larger than those calculated by B3LYP. We find that the bond constant and the differences between copper and axial methionine in the oxidized state are very significant, and the differences of the bond constants in MCOs, azurin, and stellacyanin are $28.38 \text{ kcal/mol}\cdot\text{\AA}^2$, $20.91 \text{ kcal/mol}\cdot\text{\AA}^2$, and $26.48 \text{ kcal/mol}\cdot\text{\AA}^2$, respectively.

Since the larger bond constant represents the stronger interaction of the bond, M06 represents the interaction between copper and ligand in a stronger way. A significant contribution of M06 is revealed in the case of long-range interaction between copper and axial ligand. Although the bond distance between copper and axial ligand is significantly larger than the other bonds, the interaction is still considered as a covalent bond. Hence, the calculation method that is used to investigate this interaction should be able to account long-range interaction as well. From the results, we find that M06 performs better than B3LYP in accounting the long-range interaction. One of the reasons is the implementation of meta-GGA functional, instead of pure GGA, in exchange functional of M06. The inclusion of kinetic energy density in exchange functional seems to contribute in improving DFT calculation. The other reason is related to the ratio between HF and (meta)-GGA exchange functionals and also the optimization of parameter.

The angle constants of T1Cu in MCOs, azurin and stellacyanin are provided in Tables 7, 8 and 9, respectively. In the matter of angle constants, we do not find any systematic contribution of DFT functional. By comparing to B3LYP, M06 produces the angle constants that are larger in several angles, but also smaller in another angles. This indicates that the calculation of angle constant is more complicated than the calculation of bond constant. The calculation of one angle constant cannot be purely independent from that of other angle because the change of one angle can lead to the change of other angles.

We also compare the force field of Azurin between our result and Ref. [38] as shown in Tables 5 and 8. In the case of equilibrium bond distance and equilibrium angle distance, our result produces the values that are quite similar to those of Ref. [38], especially to the results of the M06 calculation. Also, the bond constants obtained from our calculation are close to the reference. However, our result of angle constant is found to be deviated from the reference. This is related

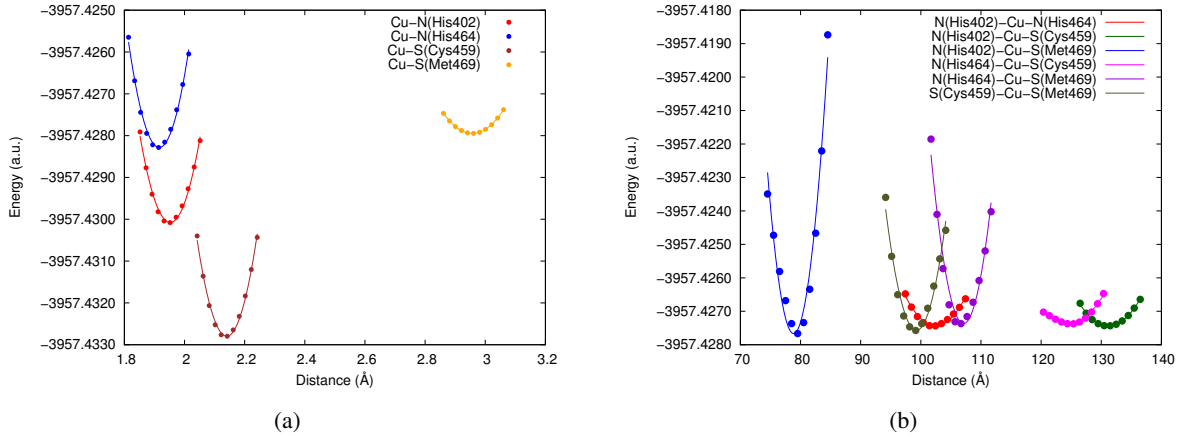


Figure 4: The potential energy surface (PES) along with (a) bond and (b) angle of oxidized state of T1Cu in MCOs protein calculated by using M06.

Table 4: The fitting parameter for bond distance the T1Cu of MCOs protein calculated by using B3LYP (M06) methods.

Bond	Reduced			Oxidized		
	r_{PDB}	r_c	K_r	r_{PDB}	r_c	K_r
Cu-N(His402)	2.072	1.99 (1.95)	104.28 (129.56)	2.01	2.00 (1.92)	89.57 (139.47)
Cu-N(His464)	1.974	1.96 (1.92)	121.49 (152.54)	2.03	1.96 (1.95)	107.79 (112.10)
Cu-S(Cys459)	2.302	2.18 (2.14)	126.97 (149.02)	2.30	2.25 (2.20)	92.3 (113.79)
Cu-S(Met469)	3.061	3.23 (2.96)	11.88 (32.57)	3.23	3.53 (3.12)	6.24 (34.62)

The units of distance (r) and force constant (K_r) are Å and kcal mol⁻¹Å⁻², respectively.

Table 5: The fitting parameter for bond distance the T1Cu of Azurin protein calculated by using B3LYP (M06) methods.

Bond	Reduced State			Oxidized State					
	r_{PDB}	r_c	K_r	r_{PDB}	r_c	K_r	r_c^a	K_r^a	
Cu-N(His46)	2.00	1.97 (1.94)	109.39 (136.66)	2.06	1.96 (1.93)	107.82 (131.11)	-	-	
Cu-N(His117)	2.11	2.00 (1.95)	106.04 (127.09)	2.19	2.05 (1.99)	72.16 (99.98)	1.948	128.45	
Cu-S(Cys112)	2.27	2.14 (2.10)	135.11 (154.38)	2.28	2.20 (2.16)	96.67 (123.98)	2.157	130.948	
Cu-S(Met121)	3.18	3.56 (3.28)	9.69 (25.80)	3.33	3.79 (3.39)	7.02 (27.93)	3.342	29.15	

^a Ref. [38]

The units of distance (r) and force constant (K_r) are Å and kcal mol⁻¹Å⁻², respectively.

to the complexity of the calculation due to the strong dependency between one angle and other angles.

The reliability of our calculation is discussed according to the comparison of the calculated results with available experimental data. In the case of maximum absorption wavelength, we find a deviation of values between our calculation and experimental data. However, the tendency of the value is a good agreement with the experimental data. This indicates that our calculation is reliable in the case of the relative value of maximum absorption wavelength. The bond distances obtained from our calculation are also quite similar to the distance obtained from the X-ray crystal structure. This points out the reliability of our calculation in predicting the bond distance around T1Cu cluster.

Table 6: The fitting parameter for bond distance of the T1Cu of Stellacyanin protein calculated by using B3LYP (M06) methods.

Bond	Reduced State			Oxidized State		
	r_{PDB}	r_c	K_r	r_{PDB}	r_c	K_r
Cu-N(His45)	1.89	1.99 (1.95)	101.46 (124.55)	2.17	2.02 (1.98)	83.15 (107.09)
Cu-N(His91)	2.06	2.05 (2.00)	99.84 (123.56)	2.06	2.05 (1.99)	85.78 (110.74)
Cu-S(Cys86)	2.23	2.18 (2.13)	128.73 (158.12)	2.24	2.22 (2.17)	92.33 (117.53)
Cu-O(Gln96)	2.22	2.41 (2.28)	29.21 (43.68)	2.52	2.83 (2.51)	9.55 (36.03)

The units of distance (r) and force constant (K_r) are Å and kcal mol⁻¹Å⁻², respectively.

Table 7: The fitting parameter for angle distance of the T1Cu of MCOs protein calculated by using B3LYP (M06) methods.

Angle	Reduced State			Oxidized State		
	θ_{PDB}	θ_c	K_θ	θ_{PDB}	θ_c	K_θ
N(His402)-Cu-N(His464)	103	102 (102)	93 (72)	105	105 (105)	78 (60)
N(His402)-Cu-S(Cys459)	129	131 (131)	93 (59)	126	130 (126)	69 (62)
N(His402)-Cu-S(Met469)	79	78 (79)	419 (529)	78	76 (77)	359 (74)
N(His464)-Cu-S(Cys459)	124	120 (124)	36 (50)	128	121 (106)	26 (109)
N(His464)-Cu-S(Met469)	107	107 (107)	375 (355)	102	102 (102)	370 (348)
S(Cys459)-Cu-S(Met469)	100	100 (99)	236 (284)	100	100 (99)	174 (246)
Cu-N(His402)-C _ε	125	123 (125)	94 (86)	127	125 (128)	89 (93)
Cu-N(His402)-C _γ	124	126 (124)	98 (93)	125	127 (124)	90 (94)
Cu-N(His464)-C _ε	125	125 (127)	205 (280)	127	127 (129)	210 (240)
Cu-N(His464)-C _γ	125	126 (124)	204 (278)	125	125 (123)	202 (227)
Cu-S(Cys459)-C _β	100	105 (100)	43 (92)	100	103 (98)	40 (84)
Cu-S(Met469)-C _ε	104	102 (103)	181 (188)	103	101 (102)	153 (127)
Cu-S(Met469)-C _γ	140	141 (140)	240 (314)	141	143 (141)	190 (324)

The units of angle (θ) and force constant (K_θ) are (°) and kcal mol⁻¹rad⁻², respectively.

4 Conclusion

We have presented a cluster model representing type I copper (T1Cu) center of several copper proteins, i.e. multicopper oxidases (MCOs), azurin and stellacyanin. Several physical properties such as atomic partial charge, atomic partial spin, ionization potential of reduced T1Cu, electron affinity of oxidized T1Cu, bond and the angle constants, etc. have been discussed in relation to DFT functionals dependency by utilizing two typical DFT functionals, i.e. B3LYP and M06. We have found the dependency of atomic partial charge and partial spin of T1Cu cluster on the DFT functionals, which correspond to electron delocalization between Cu and cysteine's sulfur and thus lead the increasing of t/U ratio in simple Hubbard model. The ionization potential (IP) of reduced T1Cu and the electron affinity (EA) of oxidized T1Cu have been approximately calculated with the present cluster model and the dependency on DFT functional have been revealed. We have also calculated the absorption wavelength of T1Cu and compared the results with experimental data. A significant contribution of M06 in the case of bond constant has been unveiled, especially in long-range interaction between copper ion and axial ligand. We have found that the interaction between copper ion and ligand is improved when M06 is adopted.

Table 8: The fitting parameter for angle distance of the T1Cu of Azurin protein calculated by using B3LYP (M06) methods.

Angle	Reduced State			Oxidized State			θ_c^a	K_θ^a
	θ_{PDB}	θ_c	K_θ	θ_{PDB}	θ_c	K_θ		
N(His46)-Cu-N(His117)	104	105 (100)	64 (93)	103	103 (105)	68 (70)	-	-
N(His46)-Cu-S(Cys112)	132	139 (145)	54 (103)	133	139 (137)	43 (58)	-	-
N(His46)-Cu-S(Met121)	75	73 (73)	558 (589)	73	70 (71)	478 (457)	-	-
N(His117)-Cu-S(Cys112)	124	116 (110)	44 (101)	123	115 (113)	34 (44)	120	12
N(His117)-Cu-S(Met121)	84	88 (88)	406 (367)	88	91 (91)	387 (413)	88	112
S(Cys112)-Cu-S(Met121)	110	110 (109)	208 (287)	112	113 (112)	155 (218)	111	96
Cu-N(His46)-C $_\epsilon$	124	121 (123)	103 (104)	126	125 (128)	105 (128)	-	-
Cu-N(His46)-C $_\gamma$	132	135 (133)	103 (104)	130	131 (128)	104 (132)	-	-
Cu-N(His117)-C $_\epsilon$	124	121 (122)	217 (334)	128	124 (126)	215 (322)	-	-
Cu-N(His117)-C $_\gamma$	129	133 (131)	188 (227)	127	131 (129)	205 (304)	-	-
Cu-S(Cys112)-C $_\beta$	109	107 (103)	88 (157)	108	106 (102)	75 (128)	108	35
Cu-S(Met121)-C $_\epsilon$	99	97 (97)	425 (430)	98	95 (95)	342 (349)	-	-
Cu-S(Met121)-C $_\gamma$	138	142 (142)	245 (236)	137	142 (141)	134 (161)	-	-

^a Ref. [38]The units of angle (θ) and force constant (K_θ) are ($^\circ$) and kcal mol⁻¹rad⁻², respectively.

Table 9: The fitting parameter for angle distance of the T1Cu of Stellacyanin protein calculated by using B3LYP (M06) methods.

Angle	Reduced State			Oxidized State		
	θ_{PDB}	θ_c	K_θ	θ_{PDB}	θ_c	K_θ
N(His45)-Cu-N(His91)	100	97 (98)	212 (213)	98	95 (97)	130 (136)
N(His45)-Cu-S(Cys86)	128	131 (135)	84 (88)	132	134 (137)	63 (72)
N(His45)-Cu-S(Met96)	94	91 (92)	367 (400)	87	83 (85)	290 (319)
N(His91)-Cu-S(Cys86)	126	116 (116)	39 (34)	125	118 (102)	26 (148)
N(His91)-Cu-O(Gln96)	95	98 (98)	513 (529)	90	92 (92)	522 (518)
S(Cys86)-Cu-O(Gln96)	105	105 (104)	295 (394)	111	112 (111)	184 (313)
Cu-N(His45)-C $_\epsilon$	121	121 (122)	95 (102)	128	125 (128)	52 (61)
Cu-N(His45)-C $_\gamma$	129	130 (128)	95 (102)	122	126 (122)	54 (65)
Cu-N(His91)-C $_\epsilon$	127	123 (125)	297 (383)	126	122 (124)	257 (404)
Cu-N(His91)-C $_\gamma$	123	127 (126)	294 (376)	123	127 (125)	248 (384)
Cu-S(Cys86)-C $_\beta$	108	109 (105)	77 (178)	108	110 (106)	73 (126)
Cu-O(Glu96)-C $_\delta$	117	115 (115)	365 (364)	106	104 (103)	260 (256)

The units of angle (θ) and force constant (K_θ) are ($^\circ$) and kcal mol⁻¹rad⁻², respectively.

References

- [1] P. M. Colman, H. C. Freeman, J. M. Guss, M. Murata, V. A. Norris, J. a. M. Ramshaw, and M. P. Venkatappa, "X-ray crystal structure analysis of plastocyanin at 2.7 Å resolution," *Nature*, vol. 272, pp. 319–324, Mar. 1978.
- [2] E. T. Adman and L. H. Jensen, "Structural Features of Azurin at 2.7 Å Resolution," *Israel Journal of Chemistry*, vol. 21, pp. 8–12, Jan. 1981.
- [3] K. Paraskevopoulos, M. Sundararajan, R. Surendran, M. A. Hough, R. R. Eady, I. H. Hillier, and S. S. Hasnain, "Active site structures and the redox properties of blue copper proteins: atomic resolution structure of azurin II and electronic structure calculations of azurin, plastocyanin and stellacyanin," *Dalton Trans.*, pp. 3067–3076, June 2006.

- [4] E. I. Solomon, M. J. Baldwin, and M. D. Lowery, "Electronic structures of active sites in copper proteins: contributions to reactivity," *Chem. Rev.*, vol. 92, pp. 521–542, June 1992.
- [5] M. M. Harding, M. W. Nowicki, and M. D. Walkinshaw, "Metals in protein structures: a review of their principal features," *Crystallography Reviews*, vol. 16, pp. 247–302, Oct. 2010.
- [6] D. E. Heppner, C. H. Kjaergaard, and E. I. Solomon, "Mechanism of the Reduction of the Native Intermediate in the Multicopper Oxidases: Insights into Rapid Intramolecular Electron Transfer in Turnover," *J. Am. Chem. Soc.*, vol. 136, pp. 17788–17801, Dec. 2014.
- [7] T. Sakurai and K. Kataoka, "Structure and function of type I copper in multicopper oxidases," *Cellular and Molecular Life Sciences*, vol. 64, p. 2642, July 2007.
- [8] R. A. Holwerda, S. Wherland, and a. H. B. Gray, "Electron Transfer Reactions of Copper Proteins," *Annual Review of Biophysics and Bioengineering*, vol. 5, no. 1, pp. 363–396, 1976.
- [9] E. I. Solomon, J. W. Hare, D. M. Dooley, J. H. Dawson, P. J. Stephens, and H. B. Gray, "Spectroscopic studies of stellacyanin, plastocyanin, and azurin. Electronic structure of the blue copper sites," *J. Am. Chem. Soc.*, vol. 102, pp. 168–178, Jan. 1980.
- [10] D. R. McMillin and M. C. Morris, "Further perspectives on the charge transfer transitions of blue copper proteins and the ligand moieties in stellacyanin," *Proceedings of the National Academy of Sciences of the United States of America*, vol. 78, pp. 6567–6570, Nov. 1981.
- [11] E. Bouwman, W. L. Driessen, and J. Reedijk, "Model systems for type I copper proteins: structures of copper coordination compounds with thioether and azole-containing ligands," *Coordination Chemistry Reviews*, vol. 104, pp. 143–172, July 1990.
- [12] D. Qiu, S. Dong, J. Ybe, M. Hecht, and T. G. Spiro, "Variations in the Type I Copper Protein Coordination Group: Resonance Raman Spectrum of ^{34}S -, ^{65}Cu -, and ^{15}N -Labeled Plastocyanin," *Journal of the American Chemical Society*, vol. 117, pp. 6443–6446, June 1995.
- [13] E. I. Solomon, U. M. Sundaram, and T. E. Machonkin, "Multicopper Oxidases and Oxygenases," *Chem. Rev.*, vol. 96, pp. 2563–2606, Nov. 1996.
- [14] E. I. Solomon, P. Chen, M. Metz, S.-K. Lee, and A. E. Palmer, "Oxygen Binding, Activation, and Reduction to Water by Copper Proteins," *Angew. Chem. Int. Ed. Engl.*, vol. 40, pp. 4570–4590, Dec. 2001.
- [15] N. Hakulinen, L.-L. Kiiskinen, K. Kruus, M. Saloheimo, A. Paananen, A. Koivula, and J. Rouvinen, "Crystal structure of a laccase from *Melanocarpus albomyces* with an intact trinuclear copper site," *Nature Structural & Molecular Biology*, vol. 9, pp. 601–605, Aug. 2002.
- [16] K. Piontek, M. Antorini, and T. Choinowski, "Crystal Structure of a Laccase from the Fungus *Trametes versicolor* at 1.90-Å Containing a Full Complement of Coppers," *Journal of Biological Chemistry*, vol. 277, pp. 37663–37669, Oct. 2002.
- [17] S. A. Roberts, A. Weichsel, G. Grass, K. Thakali, J. T. Hazzard, G. Tollin, C. Rensing, and W. R. Montfort, "Crystal structure and electron transfer kinetics of CueO, a multicopper oxidase required for copper homeostasis in *Escherichia coli*," *PNAS*, vol. 99, pp. 2766–2771, Mar. 2002.
- [18] S. Shleev, J. Tkac, A. Christenson, T. Ruzgas, A. I. Yaropolov, J. W. Whittaker, and L. Gorton, "Direct electron transfer between copper-containing proteins and electrodes," *Biosensors and Bioelectronics*, vol. 20, pp. 2517–2554, June 2005.
- [19] M. Ferraroni, N. M. Myasoedova, V. Schmatchenko, A. A. Leontievsky, L. A. Golovleva, A. Scozzafava, and F. Briganti, "Crystal structure of a blue laccase from *Lentinus tigrinus*: evidences for intermediates in the molecular oxygen reductive splitting by multicopper oxidases," *BMC Structural Biology*, vol. 7, p. 60, 2007.
- [20] T. Sakurai and K. Kataoka, "Basic and applied features of multicopper oxidases, CueO, bilirubin oxidase, and laccase," *Chem Record*, vol. 7, pp. 220–229, Jan. 2007.
- [21] J. Yoon and E. I. Solomon, "Electronic structures of exchange coupled trigonal trimeric Cu(II) complexes: Spin frustration, antisymmetric exchange, pseudo-A terms, and their relation to O₂ activation in the multicopper oxidases," *Coordination Chemistry Reviews*, vol. 251, pp. 379–400, Feb. 2007.
- [22] L. Quintanar, C. Stoj, A. B. Taylor, P. J. Hart, D. J. Kosman, and E. I. Solomon, "Shall We Dance? How A Multicopper Oxidase Chooses Its Electron Transfer Partner," *Accounts of Chemical Research*, vol. 40, pp. 445–452, June 2007.
- [23] J. Yoon, B. D. Liboiron, R. Sarangi, K. O. Hodgson, B. Hedman, and E. I. Solomon, "The two oxidized forms of the trinuclear Cu cluster in the multicopper oxidases and mechanism for the decay of the native intermediate," *Proceedings of the National Academy of Sciences*, vol. 104, pp. 13609–13614, Aug. 2007.

- [24] K. Kataoka, H. Komori, Y. Ueki, Y. Konno, Y. Kamitaka, S. Kurose, S. Tsujimura, Y. Higuchi, K. Kano, D. Seo, and T. Sakurai, "Structure and Function of the Engineered Multicopper Oxidase CueO from *Escherichia coli*—Deletion of the Methionine-Rich Helical Region Covering the Substrate-Binding Site," *Journal of Molecular Biology*, vol. 373, pp. 141–152, Oct. 2007.
- [25] K. Y. Djoko, L. X. Chong, A. G. Wedd, and Z. Xiao, "Reaction Mechanisms of the Multicopper Oxidase CueO from *Escherichia coli* Support Its Functional Role as a Cuprous Oxidase," *Journal of the American Chemical Society*, vol. 132, pp. 2005–2015, Feb. 2010.
- [26] A. J. Augustine, C. Kjaergaard, M. Qayyum, L. Ziegler, D. J. Kosman, K. O. Hodgson, B. Hedman, and E. I. Solomon, "Systematic Perturbation of the Trinuclear Copper Cluster in the Multicopper Oxidases: The Role of Active Site Asymmetry in Its Reduction of O₂ to H₂O," *Journal of the American Chemical Society*, vol. 132, pp. 6057–6067, May 2010.
- [27] H. Komori, R. Sugiyama, K. Kataoka, K. Miyazaki, Y. Higuchi, and T. Sakurai, "New insights into the catalytic active-site structure of multicopper oxidases," *Acta Crystallogr. D Biol. Crystallogr.*, vol. 70, pp. 772–779, Mar. 2014.
- [28] I. Pardo and S. Camarero, "Laccase engineering by rational and evolutionary design," *Cellular and Molecular Life Sciences*, vol. 72, no. 5, pp. 897–910, 2015.
- [29] E. I. Solomon, R. K. Szilagy, S. DeBeer George, and L. Basumallick, "Electronic Structures of Metal Sites in Proteins and Models: Contributions to Function in Blue Copper Proteins," *Chem. Rev.*, vol. 104, pp. 419–458, Feb. 2004.
- [30] S. Corni, F. De Rienzo, R. Di Felice, and E. Molinari, "Role of the electronic properties of azurin active site in the electron-transfer process," *International Journal of Quantum Chemistry*, vol. 102, pp. 328–342, Jan. 2005.
- [31] M. Pavelka and J. V. Burda, "Computational study of redox active centres of blue copper proteins: a computational DFT study," *Molecular Physics*, vol. 106, pp. 2733–2748, Dec. 2008.
- [32] D. Robinson and N. A. Besley, "Modelling the spectroscopy and dynamics of plastocyanin," *Phys Chem Chem Phys*, vol. 12, pp. 9667–9676, Sept. 2010.
- [33] Y. Zhao and D. G. Truhlar, "The M06 suite of density functionals for main group thermochemistry, thermochemical kinetics, noncovalent interactions, excited states, and transition elements: two new functionals and systematic testing of four M06-class functionals and 12 other functionals," *Theor Chem Account*, vol. 120, pp. 215–241, July 2007.
- [34] Y. Zhao and D. G. Truhlar, "Computational characterization and modeling of buckyball tweezers: density functional study of concave-convex $\pi \cdots \pi$ interactions," *Phys. Chem. Chem. Phys.*, vol. 10, pp. 2813–2818, May 2008.
- [35] U. Warde, L. Rhyman, P. Ramasami, and N. Sekar, "DFT Studies of the Photophysical Properties of Fluorescent and Semiconductor Polycyclic Benzimidazole Derivatives," *J Fluoresc*, vol. 25, pp. 685–694, Mar. 2015.
- [36] Y. Minenkov, Å. Singstad, G. Occhipinti, and V. R. Jensen, "The accuracy of DFT-optimized geometries of functional transition metal compounds: a validation study of catalysts for olefin metathesis and other reactions in the homogeneous phase," *Dalton Trans.*, vol. 41, Apr. 2012.
- [37] D. Coskun, S. V. Jerome, and R. A. Friesner, "Evaluation of the Performance of the B3lyp, PBE0, and M06 DFT Functionals, and DBLOC-Corrected Versions, in the Calculation of Redox Potentials and Spin Splittings for Transition Metal Containing Systems," *J. Chem. Theory Comput.*, vol. 12, pp. 1121–1128, Mar. 2016.
- [38] T. Shuku, K. Sugimori, A. Sugiyama, H. Nagao, T. Sakurai, and K. Nishikawa, "Molecular orbital analysis of active site of oxidized azurin: Dependency of electronic properties on molecular structure," *Polyhedron*, vol. 24, pp. 2665–2670, Nov. 2005.
- [39] A. Sugiyama, K. Sugimori, T. Shuku, T. Nakamura, H. Saito, H. Nagao, H. Kawabe, and K. Nishikawa, "Electronic structure of the active site with two configurations of azurin," *Int. J. Quantum Chem.*, vol. 105, pp. 588–595, Jan. 2005.
- [40] K. Sugimori, T. Shuku, A. Sugiyama, H. Nagao, T. Sakurai, and K. Nishikawa, "Solvent effects on electronic structure of active site of azurin by polarizable continuum model," *Polyhedron*, vol. 24, pp. 2671–2675, Nov. 2005.
- [41] M. J. Frisch, G. W. Trucks, H. B. Schlegel, G. E. Scuseria, M. A. Robb, J. R. Cheeseman, G. Scalmani, V. Barone, B. Mennucci, G. A. Petersson, H. Nakatsuji, M. Caricato, X. Li, H. P. Hratchian, A. F. Izmaylov, J. Bloino, G. Zheng, J. L. Sonnenberg, M. Hada, M. Ehara, K. Toyota, R. Fukuda, J. Hasegawa, M. Ishida, T. Nakajima, Y. Honda, O. Kitao, H. Nakai, T. Vreven, J. A. Montgomery, J. E. Peralta, F. Ogliaro, M. Bearpark, J. J. Heyd, E. Brothers, K. N. Kudin, V. N. Staroverov, R. Kobayashi, J. Normand, K. Raghavachari, A. Rendell, J. C. Burant,

- S. S. Iyengar, J. Tomasi, M. Cossi, N. Rega, J. M. Millam, M. Klene, J. E. Knox, J. B. Cross, V. Bakken, C. Adamo, J. Jaramillo, R. Gomperts, R. E. Stratmann, O. Yazyev, A. J. Austin, R. Cammi, C. Pomelli, J. W. Ochterski, R. L. Martin, K. Morokuma, V. G. Zakrzewski, G. A. Voth, P. Salvador, J. J. Dannenberg, S. Dapprich, A. D. Daniels, O. Farkas, J. B. Foresman, J. V. Ortiz, J. Cioslowski, and D. J. Fox, "Gaussian 09, Revision E.01," 2009.
- [42] H. Nar, A. Messerschmidt, R. Huber, M. van de Kamp, and G. W. Canters, "Crystal structure analysis of oxidized *Pseudomonas aeruginosa* azurin at pH 5.5 and pH 9.0: A pH-induced conformational transition involves a peptide bond flip," *Journal of Molecular Biology*, vol. 221, pp. 765–772, Oct. 1991.
- [43] M. Koch, M. Velarde, M. D. Harrison, S. Echt, M. Fischer, A. Messerschmidt, and C. Dennison, "Crystal structures of oxidized and reduced stellacyanin from horseradish roots," *Journal of the American Chemical Society*, vol. 127, pp. 158–166, Jan. 2005.
- [44] H. Nar, *Röntgenkristallographische Strukturaufklärung Von Azurin Aus Pseudomonas Aeruginosa*. PhD thesis, 1992.
- [45] U. C. Singh and P. A. Kollman, "An approach to computing electrostatic charges for molecules," *J. Comput. Chem.*, vol. 5, pp. 129–145, Apr. 1984.
- [46] B. Mennucci, "Polarizable continuum model," *WIREs Comput Mol Sci*, vol. 2, pp. 386–404, May 2012.
- [47] T. V. Harris and R. K. Szilagy, "Protein environmental effects on iron-sulfur clusters: A set of rules for constructing computational models for inner and outer coordination spheres," *J. Comput. Chem.*, vol. 37, pp. 1681–1696, July 2016.
- [48] C. Liu, B. Zhang, Y. Zhu, and M. Tang, "Evaluations of AMBER force field parameters by MINA approach for copper-based nucleases," *Struct Chem*, pp. 1–16, May 2016.